

# Asymmetric QWS DFB Laser Diodes

Carlos Ferreira Fernandes

**Abstract**—Quarterly wavelength shifted (QWS) distributed feedback (DFB) laser structures are commonly referred to be associated with high mode selectivity, zero-frequency detuning and small threshold current density. The present paper compares different asymmetric QWS structures in the threshold regime, the results being summarized to show their influence on the emission laser characteristics.

**Index Terms** — Matricial Techniques, DFB Lasers, Single Longitudinal Mode Operation .

## I. INTRODUCTION

Lasers suitable for high bit rate transmission systems are requested to present single longitudinal mode (SLM) operation. According to the coupling wave theory [1], the electric field distribution along the cavity may be defined according to the amplitude of two counter-running waves. They are coupled with each other by the corrugation, whose amplitude is defined by the coupling coefficient. The laser emission features are seen to be strongly dependent on the conditions assumed at the cavity ends. Due to the tolerances generally associated with the facet ends [2], these ones are often coated with anti-reflexive (AR) films. However, the symmetric structure of these mirrorless cavities is associated with double degenerate patterns, which prevent the SLM operation [3]. To overcome this problem, several modified DFB structures have been proposed [4-6], the most popular of them corresponding to the introduction of a phase-shift of  $\pi/2$  within the corrugation. It is commonly referred as the  $\lambda/4$  shifted or quarterly shifted (QWS) laser [7]. The phase-shift introduces a mode in the Bragg wavelength, which may be or not the main mode, depending on its location inside the cavity. At threshold for the symmetric structure (PS at the center of the cavity) the laser presents the highest mode selectivity and the smallest current density, besides a zero-frequency detuning. However, the related electric field distribution is highly non-uniform, especially for high coupling, presenting a strong peak near the center. This is responsible for a quick degradation of the laser performance in the high power regime (spatial hole-burning effect [8]). Several methods for

obtaining asymmetric structures are proposed, namely: (i) lasers with the  $\lambda/4$  PS moved away from the centre, (ii) different coupling coefficients related to the corrugation in each side of the PS or (iii) strongly asymmetric end facet reflectivities. This work shows their influences on the main emission properties of the light source using matrix techniques [9], which seem to be especially adequate to deal with those situations.

## II. MODEL DESCRIPTION

In the present analysis the calculations use the transfer matrix formalism. The main point is the description of the laser cavity by a finite number of cells, representing the corrugation and the facets. On both sides of each cell the right and left going waves,  $\mathbf{u}$  and  $\mathbf{v}$ , are related by two linear equations. Each cell will then be represented by a  $2 \times 2$  complex matrix. The input data are the Bragg wavelength,  $\lambda_B$ , the coupling coefficient,  $K_C$ , the effective refractive index,  $n_{ef}$ , the cavity length,  $L$ , and the reflectivities,  $R_R$  and  $R_L$ , plus phase shifts,  $\phi_R$  and  $\phi_L$ , on both ends.

The corrugation corresponds to a periodic variation of the refractive index with period  $\Lambda=2l$ , where its characteristic parameters are:

$$\ell = \frac{\lambda_B}{4n_{ef}} \quad (1)$$

$$n_1 = n_{ef} - \frac{K_C \lambda_B}{4} \quad (2)$$

$$n_2 = n_{ef} + \frac{K_C \lambda_B}{4} \quad (3)$$

The matrix associated to one period of the corrugation, symmetrically placed with regard to the cavity ends, is:

$$[M_\Lambda] = \frac{1}{1-r^2} \begin{bmatrix} e^{-j\Gamma_A \ell} - r^2 e^{j\Gamma_B \ell} & r(e^{-j\Gamma_2 \ell} - e^{j\Gamma_2 \ell}) \\ r(e^{j\Gamma_2 \ell} - e^{-j\Gamma_2 \ell}) & e^{j\Gamma_A \ell} - r^2 e^{-j\Gamma_B \ell} \end{bmatrix} \quad (4)$$

where:

$$\Gamma_A = \frac{\omega}{c}(n_1 + n_2) + 2j\gamma \quad (5)$$

Manuscript received March 10, 2004. This work was supported by the Institute of Telecommunications/IST Lisbon, Portugal.

C. F. Fernandes is with the Institute of Telecommunications, Department of Electrical and Computer Engineering, Instituto Superior Técnico, Av. Rovisco Pais, 1049-001, Lisboa, Portugal. (phone: 351-21-8417971; fax: 351-21-8417672; e-mail: ffernandes@ist.utl.pt).

$$\Gamma_B = \frac{\omega}{c}(n_2 - n_1) \quad (6)$$

$$r = \frac{n_2 - n_1}{n_1 + n_2} \quad (7)$$

$$\Gamma_2 = \frac{\omega}{c}n_2 + j\gamma \quad (8)$$

The matrix related to the right facet, defined by a reflectivity  $R_R = r_R^2$  and a phase shift  $\phi_R = \pi l_R/l$ , assumes the form:

$$[M_R] = \frac{1}{\sqrt{1-r_R^2}} \begin{bmatrix} e^{-j\phi_R/2} & -r_R e^{-j\phi_R/2} \\ -r_R e^{j\phi_R/2} & e^{j\phi_R/2} \end{bmatrix} \quad (9)$$

In a similar way, the matrix related to the left facet, represented by  $R_L$  and  $\phi_L$ , is:

$$[M_L] = \frac{1}{\sqrt{1-r_L^2}} \begin{bmatrix} e^{-j\phi_L/2} & r_L e^{-j\phi_L/2} \\ r_L e^{j\phi_L/2} & e^{j\phi_L/2} \end{bmatrix} \quad (10)$$

In this formalism the facets may be represented by two cells of length  $l_R$  and  $l_L$  and the counter-propagating waves are related by the matrices  $[M_R]$  and  $[M_L]$ . Due to the fact that  $l_R, l_L \ll L$ , the attenuation imposed by the facets is neglected. In conventional DFB laser diodes the matrix  $[M]$  is simply the product of the partial matrices related to the facets plus corrugation:

$$[M] = [M_R][M_{cor}][M_L] \quad (11)$$

$$[M_{cor}] = \prod_{i=1}^N [M_i] = \prod_{i=1}^N [M_\Lambda]^{m_i} \quad (12)$$

where  $m_i$  is the number of periods inside the  $i$ th cell and  $N$  the number of cells within the cavity.

In symmetric structures and in the absence of non-uniformities associated with spatial variations of the photon and carrier populations, the matrix related to each cell is invariant. Residue phases at the facets make the spectrum asymmetric with respect to the Bragg frequency, even if the reflectivities have the same value at both ends. In mirrorless DFB structures the laser spectrum becomes doubly degenerate, not allowing the oscillation at the Bragg wavelength and it does not depend on the facet phase shifts. Thus the SLM operation becomes not feasible. The introduction of phase shifts along the corrugation overcomes this problem. Phase shift gratings are easily included using the matrix formalism. Assuming a small electric field discontinuity along the plane of the phase shift located at  $z_\phi$ ,

the related matrix is:

$$\begin{bmatrix} \mathbf{u}(z_\phi^+) \\ \mathbf{v}(z_\phi^+) \end{bmatrix} = [M_\phi] \begin{bmatrix} \mathbf{u}(z_\phi^-) \\ \mathbf{v}(z_\phi^-) \end{bmatrix} = \begin{bmatrix} e^{j\phi} & 0 \\ 0 & e^{-j\phi} \end{bmatrix} \begin{bmatrix} \mathbf{u}(z_\phi^-) \\ \mathbf{v}(z_\phi^-) \end{bmatrix} \quad (13)$$

Owing to the conservation of energy, the matrix  $[M]$  as well as its inverse must satisfy the reciprocity rule:

$$M_{11}M_{22} - M_{12}M_{21} = 0 \quad (14)$$

The oscillation condition corresponds to the vanishing of the incoming waves and it is given by the complex equation:

$$M_{22}(\delta\beta, \gamma) = 0 \quad (15)$$

Equation (15) is solved using the Newton-Raphson technique (see appendix). The solutions are the detuning  $\delta\beta$  and the gain  $\gamma$  related to each mode that is allowed to propagate inside the cavity. The normalized gain selectivity,  $\delta\gamma L$ , corresponds to the difference between the values associated with the main side mode and the main mode. While the requirement of the gain selectivity may vary from one optical communication system to another, it is generally accepted that for cavity lengths of about 500 Å, a minimum value of 0.5 (or equivalently, a 25 dB side mode suppression ratio) shall be insured [10]. However, the non-uniformity of the electric field distribution, associated with a strong carrier injection, alters the longitudinal distribution of the refractive index, which also affects the field distribution. These effects are well known and correspond to the major drawback of this kind of lasers in the high power regime. In order to ensure a stable SLM operation, the structure must be optimized with respect to the field intensity distribution. For this purpose a parameter  $F$  (flatness) is defined, being given by:

$$F = \frac{1}{L} \int_0^L \left[ \frac{I(z)}{I_{av}} - 1 \right]^2 dz \quad (16)$$

where  $I_{av}$  is the average field intensity inside the cavity.

In order to minimize the spatial hole-burning effect, therefore improving the maximum single mode output power, it is required that  $F < 0.05$ .

The electric field intensity is proportional to the photon density which, at the end of the  $k$ th cell, is given by:

$$N_{ph_k} = C \left( |M_{12}^k|^2 + |M_{22}^k|^2 \right) \quad (17)$$

where  $[M^k]$  is the matrix that relates the waves at the  $k$ th section to those at the left facet. It is given by:

$$[M^k] = [M_k][M_{k-1}] \cdots [M_1][M_L] \quad (18)$$

and  $C$  is a normalization constant, whose value is obtained according to the steady state carrier equation. It depends on the structural parameters, namely the active layer width,  $d$ , the active layer thickness,  $w$ , and the laser cavity ends,  $L$ .

The output powers from the front and back facets are denoted by  $P_f$  and  $P_b$ , respectively, which are proportional to the photon population in the first and last cells, obtained using (17).

The external differential quantum efficiencies, denoted by  $\eta_{df}$  and  $\eta_{db}$ , are obtained from:

$$\eta_{df} = \frac{\alpha_{th}}{\alpha_{int} + \alpha_{th}} \frac{P_f}{P_f + P_b} \quad (19)$$

$$\eta_{db} = \frac{\alpha_{th}}{\alpha_{int} + \alpha_{th}} \frac{P_b}{P_f + P_b} \quad (20)$$

where  $\alpha_{th}$  is the main mode loss at threshold and  $\alpha_{int}$  represents the internal losses.

### III. RESULTS

All the results correspond to a  $\lambda/4$  InGaAsP/InP DFB laser diode whose parameters are shown in Table I. The phase shift location is defined by the parameter  $p_\phi = 2z_\phi/L$ . The front (left) facet corresponds to  $p_\phi=0$  and the rear (right) facet to  $p_\phi=2$ . The PS divides the corrugation in two parts with coupling coefficients  $K_f$  and  $K_b$  and lengths  $L_f$  and  $L_b$ . Obviously  $L_f+L_b=L$ . In the results the corrugation will be identified by the values  $K_C:K_{Cb}$  and  $L_f:L_b$  or  $p_\phi$ .

TABLE I  
MATERIAL AND STRUCTURAL PARAMETERS

Parameter	Symbol	Value	Unit
Internal losses	$\alpha_{int}$	40	$\text{cm}^{-1}$
Laser cavity length	$L$	500	$\mu\text{m}$
Active layer thickness	$w$	1.5	$\mu\text{m}$
Active layer width	$d$	0.3	$\mu\text{m}$
Confinement factor	$\Gamma$	0.66	
Bragg wavelength	$\lambda_B$	1.55	$\mu\text{m}$
Group velocity	$v_g$	$3 \times 10^8 / 3.41$	m/s

Fig.1 shows the flatness *versus* phase-shift position  $p_\phi$  for several corrugations with uniform coupling coefficients. It is apparent that increasing the coupling coefficient increases the non-uniformity of the electric field distribution, meaning worse performances in the high power regime. It is also shown that the asymmetry imposed by the PS ( $p_\phi \neq 1$ ) corresponds to a disadvantage as far as the hole-burning is

concerned. It is worth noticing that the stable SLM *criterium* is only observed for weak coupling when the PS is in the vicinity of the center of the cavity.

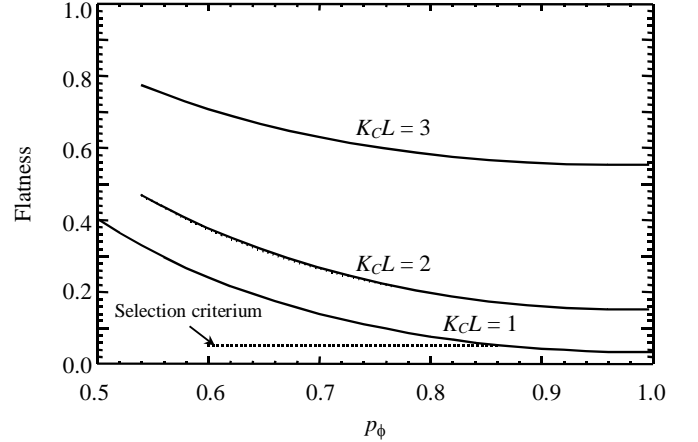


Fig. 1. Flatness as a function of the phase shift position.

Fig. 2 shows the normalized mode selectivity *versus* PS location for the same set of lasers. The gain margin increases when the PS approaches the center, the emission spectra becoming doubly degenerate for  $p_\phi$  around 0.5. The range of PS locations becomes more and more restrictive as  $K_C$  increases. Again the symmetric structure represents the most attractive option.

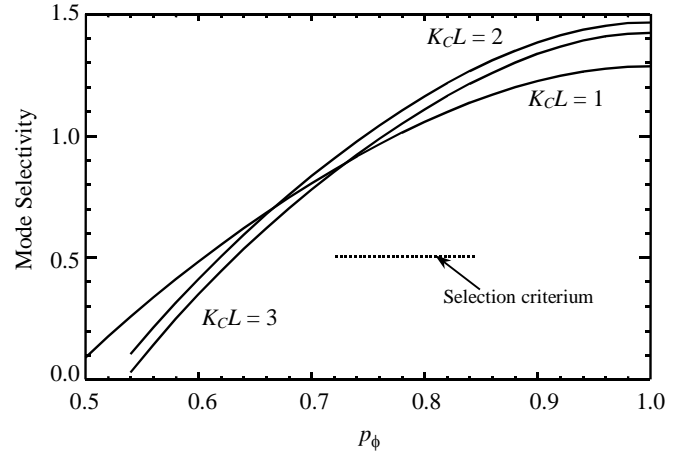


Fig. 2. Mode selectivity as a function of the phase shift position.

Fig. 3 shows the ratio between the front and back output powers *versus* PS location. The asymmetry improves the ratio  $P_f/P_b$ , the effect being particularly important for strong coupling. Obviously, for the symmetric structure ( $p_\phi=1$ )  $P_f/P_b=1$ .

Fig.4 shows the front external differential quantum efficiency of the laser structures versus PS location.

Again the asymmetry benefits the laser performance, but  $K_C$  shall be small. While increasing the front emitted power face to the back power, the increase of the coupling coefficient leads to a decrease in the threshold gain. This happens due to the high concentration of the electric field distribution near the PS for strong coupling coefficients.

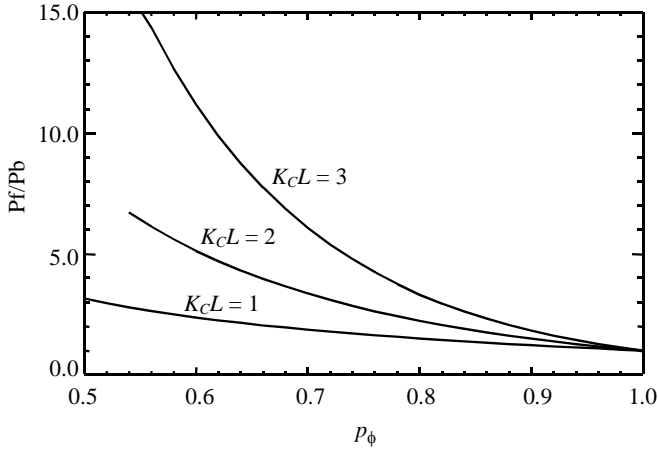


Fig. 3. Output power ratio as a function of the phase shift position.

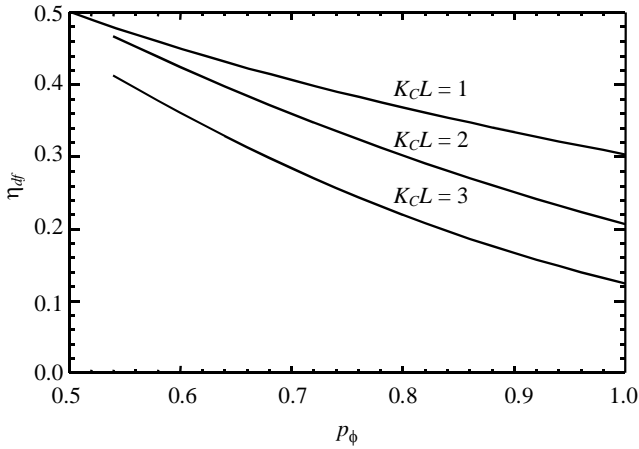


Fig. 4. External differential quantum efficiency as a function of the phase shift position.

Figs. 5-8 show the influence of the coupling coefficient variation on the emission properties of the laser.

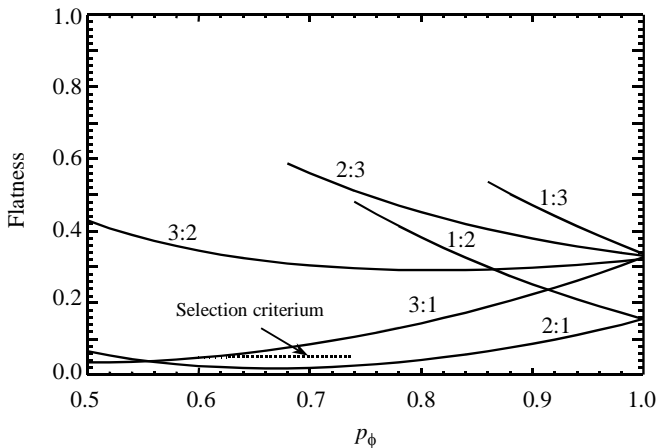


Fig. 5. Flatness versus PS location for various coupling ratios. Coupling ratio  $K_{Cf}/K_{Cb}$  is denoted by  $K_{Cf} : K_{Cb}$ .

Let's define the coupling ratio as  $K_{Cf}/K_{Cb}$ . In each figure we can see 3 curves for ratio < 1 and 3 curves for ratio > 1. Some conclusions shall be emphasized. Namely:

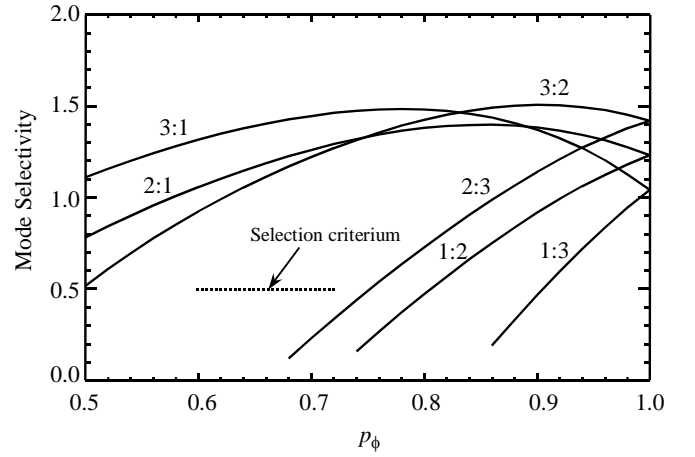


Fig. 6. Gain margin versus PS location for various coupling ratios. Coupling ratio  $K_{Cf}/K_{Cb}$  is denoted by  $K_{Cf} : K_{Cb}$ .

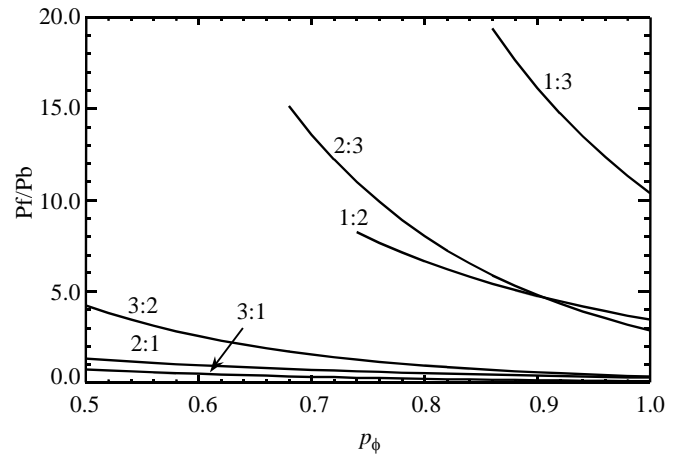


Fig. 7. Output power ratio versus PS location and coupling ratios. Coupling ratio  $K_{Cf}/K_{Cb}$  is denoted by  $K_{Cf} : K_{Cb}$ .

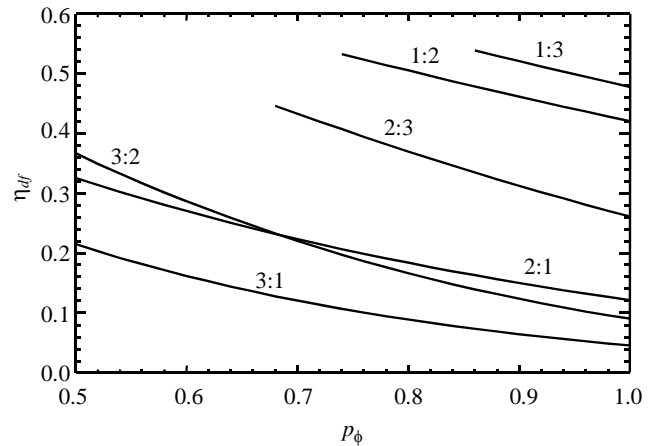


Fig. 8. Quantum efficiency versus PS location and coupling ratios. Coupling ratio  $K_{Cf}/K_{Cb}$  is denoted by  $K_{Cf} : K_{Cb}$ .

(i) In the symmetric structure ( $p_\phi=1$ ) the flatness and the gain selectivity are the same for  $r$  and  $1/r$ .

(ii) In the symmetric case the value of  $P_f/P_b$  for  $r$  is inverse of the one obtained for  $1/r$ .

(iii) For  $r < 1$  the spectra are doubly degenerate as the PS approaches the front facet. For  $r > 1$  the SLM operation is always ensured in the range under analysis.

(iv) The advantages of  $r > 1$  is twofold: smaller values of flatness and greater gain margins.

(v) However, when  $r > 1$  the lasers present small differential quantum efficiencies, since  $P_f < P_b$  for all PS positions.

Finally the influence of the conditions assumed at the cavity ends was considered. The results are presented in the figures 9 to 12. The power reflectivity was taken as 0.25 per cent for both facets. The dashed zones correspond to the spread obtained when the facet phase shifts are allowed to vary along their entire range. As we can see their influence decreases as the coupling coefficient becomes higher, meaning that the emission properties are mainly defined by the corrugation properties.

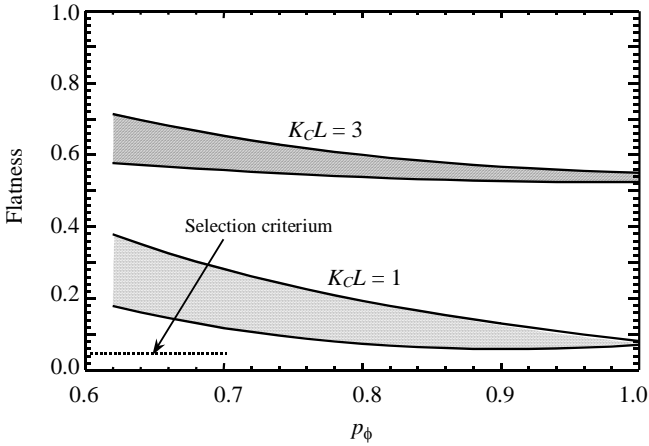


Fig. 9. Flatness versus PS position for different coupling strength and phase shifts at cavity facets.

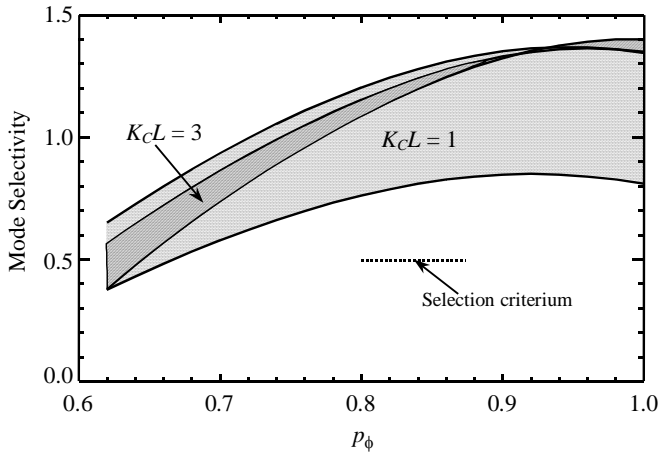


Fig. 10. Mode selectivity versus PS position for different coupling strength and phase shifts at cavity facets.

In strongly asymmetric DFB structures with weak coupling strength high gain margins may be obtained while maintaining high values for output power ratios and quantum efficiencies.

Results obtained are in full agreement with those referred in [11].

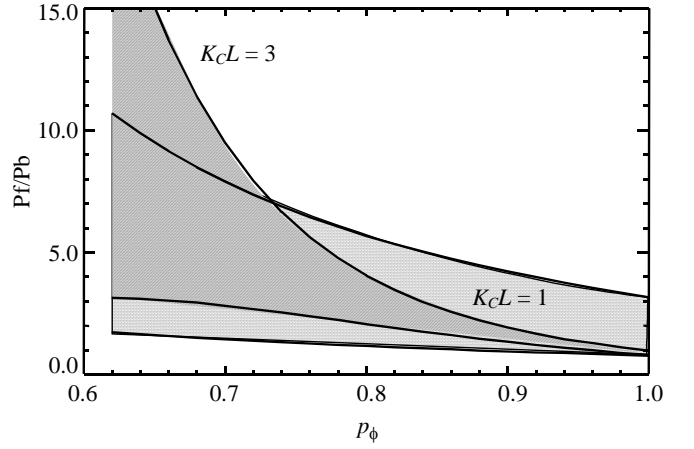


Fig. 11. Output power ratio versus PS position for different coupling strength and phase shifts at cavity facets.

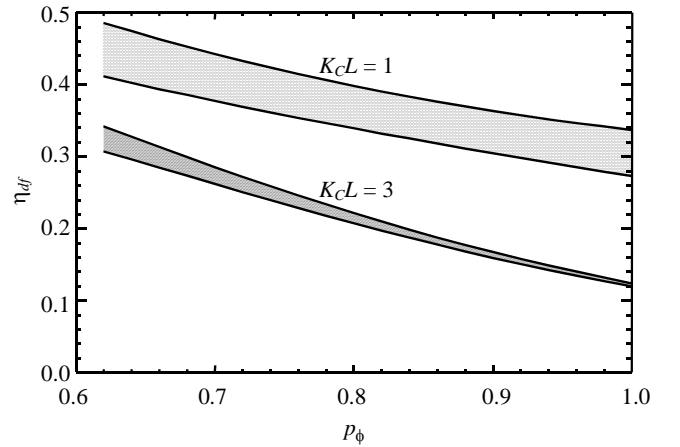


Fig. 12. Quantum efficiency versus PS position for different coupling strength and phase shifts at cavity facets

#### IV. CONCLUSIONS

Asymmetric QWS DFB laser diodes were analyzed. In AR coated lasers the output power ratios and the quantum differential efficiencies are increased as the PS approaches the front facet. The SLM operation is reached if  $0.6 < p_\phi < 1$ . The corresponding quantum efficiencies are between 30% (for the symmetric case) and 45% (for lasers with length ratio  $L_f : L_b$  equal to 30:70). In QWS DFB lasers with power reflectivities of 0.25%, only about 1/3 of the cases would ensure the SLM operation when the length ratio is 30:70, but the quantum efficiency may reach 50%.

The model used in all the calculations is based on matrix techniques. They are seen to be very flexible: laser structures are represented by the same general equation; the algorithm derived can be applied to several structures.

#### APPENDIX

$$\omega_{n+1} = \omega_n + \left[ M_{22}(2) \frac{\partial f_1}{\partial \gamma} - M_{22}(1) \frac{\partial f_2}{\partial \gamma} \right] / D \quad (A1)$$

$$\gamma_{n+1} = \gamma_n + \left[ M_{22}(1) \frac{\partial f_2}{\partial \omega} - M_{22}(2) \frac{\partial f_1}{\partial \omega} \right] / D \quad (\text{A2})$$

where  $M_{22}(1)$  and  $M_{22}(2)$  represent the real and imaginary parts of  $M_{22}$ , respectively, and:

$$M_{22}(1) = f_1(\omega_n, \gamma_n) \quad (\text{A3})$$

$$M_{22}(2) = f_2(\omega_n, \gamma_n) \quad (\text{A4})$$

$$D = \frac{\partial f_1}{\partial \omega} \frac{\partial f_2}{\partial \gamma} - \frac{\partial f_2}{\partial \omega} \frac{\partial f_1}{\partial \gamma} \quad (\text{A5})$$

$$\omega_n = \frac{c}{n_{ef}} \beta_n \quad (\text{A6})$$

$\omega_n, \gamma_n$  are the roots of (15) corresponding to the  $n$ th iteration

#### REFERENCES

- [1] H. Kogelnik and C.V. Shank, "Coupled-Wave Theory of Distributed Feedback Lasers", *J. Appl. Phys.*, vol. 43, No. 5, pp. 23-27, 1972.
- [2] J. Buus, "Mode Selectivity in DFB Lasers with Cleaved Facets", *Electron. Letters*, vol. 21, pp. 179-180, 1985.
- [3] S.R. Chinn, "Effects of Mirror Reflectivity in a Distributed Feedback Laser", *IEEE J. Quantum Electronics*, QE-9, pp. 574-580, 1973.
- [4] P. Zhou and G.S. Lee, "Chirped Grating  $\lambda/4$  Shifted Distributed Feedback Laser with Uniform Longitudinal Field Distribution", *Electron. Letters*, vol. 26, No. 20, pp. 1660-1661, 1990.
- [5] Y. Kotaki, M. Matsuda, T. Fujii and H. Ishikawa, "MQW-DFB Lasers with Non-Uniform Depth  $\lambda/4$  Shifted Gratings", *Proc. ECOC/ICOC 91*, pp. 137-140, 1991.
- [6] G. Mortier, K. David, P. Vankwikelberge and R. Baets, "A New DFB Lasers Diode with Reduced Spatial Hole-Burning", *IEEE Photonics Techn. Lett.*, vol. 2, No. 6, pp. 388-390, 1990.
- [7] K. Utaka, S. Akita, K. Sakai and Y. Matsushima, " $\lambda/4$  shifted InGaAsP/InP DFB Laser", *IEEE J. Quantum Electronics*, QE-22, pp. 1042-1051, 1986.
- [8] H. Soda, Y. Kotaki, H. Sudo, H. Ishikawa, S. Iamakoshi, H. Imai, "Stability in Single Longitudinal Mode Operation in InGaAsP/InP Phase Adjusted DFB Lasers", *IEEE J. Quantum Electronics*, QE-23, No. 6, pp. 804-814, 1987.
- [9] C. Ferreira Fernandes, "Mode Spectrum and Threshold Gain Calculations in DFB Lasers", *Microwave Opt. Techn. Lett.*, vol. 12, No. 6, pp. 366-372, 1996.
- [10] H. Ghafouri-Shiraz and B.S.K. Lo, *Distributed Feedback Laser Diodes – Principles and Physical Modelling*, John Wiley & Sons, N.Y., Ch. 4 and 5, 1996.
- [11] M. Usami, S. Akiba and K. Utaka, "Asymmetric  $\lambda/4$  Shifted InGaAsP/InP DFB Lasers", *IEEE J. Quantum Electronics*, QE-23, No. 6, pp. 815-821, 1987.